Henry *et al. Appl Netw Sci* (2021) 6:79
https://doi.org/10.1007/s41109-021-00422-2

Applied Network Science

RESEARCH Open Access

# REINFORCE: rapid augmentation of large-scale multi-modal transport networks for resilience enhancement

Elise Henry*, Angelo Furno and Nour-Eddin El Faouzi

*Correspondence:
elise.henry@univ-eiffel.fr
ENTPE, LICIT, Univ. Gustave Eiffel, Univ. Lyon, 69675 Lyon, France

**Abstract**

With the recent and continuous growth of large metropolis, the development, management and improvement of their urban multi-modal transport networks become a compelling need. Although the creation of a new transport mode often appears as a solution, it is usually impossible to construct at once a full networked public transport. Therefore, there is a need for efficient solutions aimed at prioritizing the order of construction of the multiple lines or modes that a transport operator might want to construct to increase its offer. For this purpose, we propose in this paper a simple and quick-to-compute methodology, called REINFORCE, to prioritize the order of construction of the lines of a newly designed transport mode by maximizing the transport network performances and enhancing the transport network resilience, as described by complex networks metrics. REINFORCE could also be helpful to support the rapid and quick response to disruptions by setting up or reinforcing an adapted emergency transport line (e.g., bus service) over a set of predefined itineraries.

**Keywords:** Multi-modal transport modelling, Multi-layer networks, Transport network design

## Introduction

The continuous increase of the world's population in urban areas (Nations 2018) and the need for ensuring the urban mobility of such large volumes of people demand for adapting and augmenting the current transport offer in large agglomerations by considering the addition of new transport modes or the development of new transport lines. As highlighted by Aljoufie et al. (2011), a strong relationship exists between the urban growth and the transport network extension. The latter is also accentuated by the fact that some transport networks already operate at their capacity limits (International transport forum 2016; Dolinayova et al. 2020).

Due to the urgency of the situation and the need to stagger over time the construction of a public transport network for budget constraints and roadworks occupancy, it is essential to optimally schedule the construction of the transport network in order to quickly improve the network performances. Such analyses are at the interface of network design and graph augmentation. The first field focuses on the problems of planning and

implementing a (transport) network (Ceder and Wilson 1986). The second one aims at identifying the smallest set of edges/nodes that, once added to the input graph, improves one or more graph properties (Frank and Jordán 2015).

Our study aims at optimizing the construction in terms of short-term efficiency of a public transport network by proposing a methodology (REINFORCE) to quantify the positive impact of the addition of transport lines. The design of the new transport lines is in fact considered as a given input of the proposed methodology. Additionally, in light of an application for emergency planning (e.g., when hardly-predictable events occur), REINFORCE satisfies the requirement of quick computation to allow for a rapid definition of a provisional public transport line, such as a bus line, to be deployed over the disturbed network to properly handle the emergency situation.

This paper is an extension of our previous study (Henry et al. 2020). In the latter, we proposed an approach to summarize the main topological characteristics of a given transport network, considering the traffic conditions via a weighting process, based on the computation of multi-layer (weighted) shortest paths. Based on such model, a lightweight methodology was proposed to rank different transport line construction scenarios, based on both global and local adapted complex network metrics computed atop the proposed multi-layer modelling solution. In this paper, differently from our previous work, we integrate in our multi-layer modelling approach a more realistic solution to consider and penalize mode changes during shortest path computation, by taking into account the fact that a user aims to keep travel times low and guarantee the comfort of her travel. Secondly, we propose to include travel demand in the considered metrics to capture the importance of the most popular paths. Thirdly, we study the impact on our methodology of a special event with a significantly larger than usual public transport demand. This event permits to highlight the ability of REINFORCE to be leveraged in response to specific events in order to dynamically deploy flexible bus lines that can help in managing the emergency situation.

The main contributions of our approach can be summarized as follows: (i) we develop a quick-to-compute methodology to capture the impact of the addition of public transport lines to an existing transport network. Our approach allows identifying the lines to be constructed with highest priority, and can be adopted as well to drive the deployment process of flexible bus lines for managing a mobility-emergency situation; (ii) we propose a simplified multi-layer network modelling approach of the multi-modal transport network of a large-scale city. By using such a model we provide a holistic view of the transport system that captures most of the relevant features of a complex transport network system; (iii) we consider both network topology and traffic condition in our approach, by including both travel demand and travel time in the computation of the accessibility metrics that we use to quantify the impact on performance for given areas that derives from the addition of a transport lines.

## Literature review

The methodology presented in the paper aims both at prioritizing the construction of a new transport mode and improving the network functioning in presence of disruption by quickly commissioning new bus lines that could maximize the network performances.

### Network design to enhance the transport network resilience

Transportation networks are frequently subject to various types of disruptions such as extreme weather events, human attacks or technological failures. This may affect the performance of transportation systems which are essential for societies hence the interest of obtaining a resilient transport system. Holling (1973) first introduced this concept in ecological systems and defined it as "the ability of these systems to absorb changes of state variables, driving variables, and parameters, and still persist". In the field of transportation, two major approaches, the topological and the dynamic ones, are studied to analyse the transport network resilience to ensure acceptable levels of service under disrupted network conditions (Haimes 2009; Hassan et al. 2019).

The topological approach, based on graph theory aims at quantifying resilience by looking at the connectivity properties of the network for identifying structural criticalities (Eusgeld et al. 2009), often using centrality measures. The transport network is represented by an undirected or directed graph $G = (V, E)$, where edges ($E$) correspond to roads, and nodes ($N$) to intersections. Freiria et al. (2015) identified the most important roads in a Portuguese network by analyzing link-based topological patterns. Shalaby et al. (2016) studied the performance of public transport network in Toronto and USA. Tu et al. (2010) applied topological vulnerability indices on the Sioux Falls network (Berche et al. 2009). Based on these works from the literature, it appears reasonable to use centrality measures to quantify the impact deriving from the the addition of a transport line.

### Network performances quantification

Quantifying the performance of the multi-modal transport network, both at global and local scales, is essential to describe the positive impact determined by the construction of a novel transport line. To this purpose, we propose to firstly consider a set of quickly-to-compute global indicators to provide insights about the impact of the addition of a transport line thus allowing to rapidly select a subset of the best scenarios. Secondly, a local analysis permits to refine the previous results and describe the geographical distribution of the improvements. Two approaches in network improvement becomes possible: a higher improvement in network efficiency localized in a tight area could, for instance, be preferred to a moderate enhancement of the global performances uniformly distributed over the network. However, in this paper, the second strategy is preferred according to a resilience point of view, as it allows to increase network properties more homogeneously over the whole network. In other words, although the public transport network is simplified, each node of the graph represents most of the time a unique station (e.g., a public transport station, an inter-modal interchange, etc.). Thus, a large localized improvement of network performances, induced by the construction of a transport line, is seen as a vulnerable choice. In fact, the removal or degradation of this specific part of the network will highly negatively impact the network performances.

As will be detailed in "The REINFORCE methodology" section, the multi-modal transport network is modelled as a weighted directed multi-layer graph (Kivelä et al. 2014), $G = (V, E, L)$, with $L = \{L_m\}_{m=1}^{M}$ the set of elementary layers, each representing a specific transport mode $m$, $V$ the set of nodes and $E$ the set of edges. Each layer contains a node

subset $V_l \subset V$ and an edge one $E_l \subset E$, which correspond, respectively, to the set of intersections and the intra-layer segments composing the transport mode $m$ represented on layer $l \in L$. The edge set $E$ is also composed by inter-layer edges $E_{l'}$ that allow to cross the layers, i.e., to switch between two different transport modes composing the graph.

The different metrics adopted in our methodology, further detailed in "Global metrics" and "Local metrics" sections, have been adapted to our multi-layer modelling. In particular, we compute the importance of small geographical areas, each considered as a node in our macroscopic representation of the multi-modal transport network, through different centrality metrics. To that purpose, we consider the degree of a node $u$, i.e., $NDC_u$ (Eq. 1), as the sum of the number of edges entering into/exiting from the given geographical area, independently of the transport mode and, consequently, of their layer. We likewise consider that shortest paths can contain any edge $e \in E$ regardless of its layer, although, as further detailed in "Shortest path computation" section, inter-layer edges $E_{l'}$ are penalized during the computation of shortest paths, in order to minimize the total number of transport mode changes characterizing a given shortest path.

#### *Shortest path computation*

The shortest paths used in the studied centrality metrics are computed over our multi-layer graph model. We consider both topology and traffic conditions in the computation of the shortest paths by weighting the edges by their free flow travel time ("Introduction" section). The penalization of the inter-layer edges is induced by considering weights that are comprised between 0 and 15 min depending on the associated travel mode change, the studied area and the presence of a car park. This penalization is supposed to simulate the overhead induced by a modal switch during a multi-modal path. Using the Dijkstra's algorithm (Dijkstra 1971), we compute the (free-flow) travel time weighted shortest paths used for the calculation of our metrics.

#### *Global metrics*

The degree centrality $NDC$ (Eq. 1) distribution is an important indicator for network characterization (Costa et al. 2007; Gao and Barabási 2016; Aliakbary et al. 2018). For the sake of simplicity and despite this could represent a strong assumption, we decided to reduce this distribution by considering only its average, known as the network density ($\langle NDC \rangle$) (Eq. 2). $\langle NDC \rangle$ characterizes the nodes' connectivity in the whole network, which is an important aspect from the perspective of redundancy and capability to absorb perturbations. The denser the graph, the more connections exist between nodes. In other words, the more redundancy is provided into the network, as indicated by higher values of the average degree, the greater the level of its resilience (Zhang et al. 2015).

$$NDC_u = |E_{uv}| + |E_{vu}| \tag{1}$$

$$\langle NDC \rangle = \sum_{u \in V} \frac{NDC_u}{|V|} \tag{2}$$

where $V$ is the set of vertices, $|V|$ its cardinality and $NDC_u$ is the degree centrality of the small geographical area represented as the node $u$.

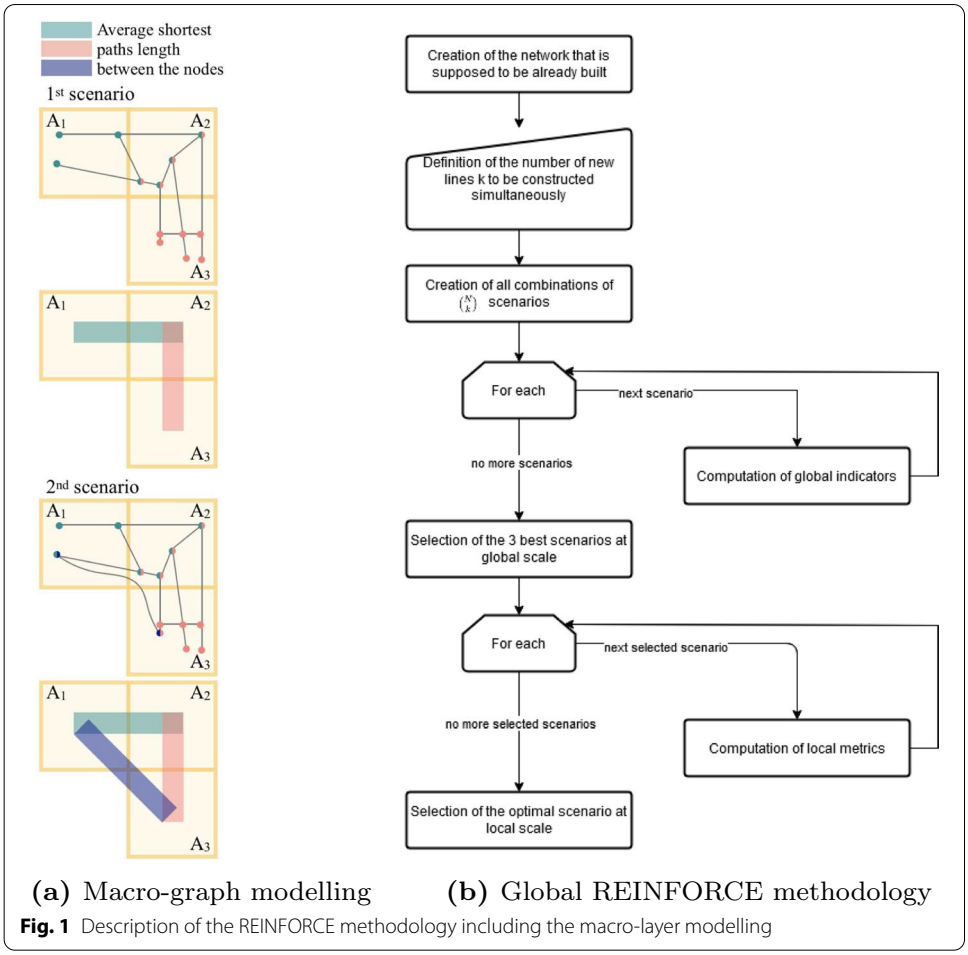


**(a)** Macro-graph modelling **(b)** Global REINFORCE methodology

**Fig. 1** Description of the REINFORCE methodology including the macro-layer modelling

We also consider the Average Efficiency (*AE*) (Eq. 3) (Latora and Marchiori 2001), frequently employed in the related literature (Bíl et al. 2015; Aydin et al. 2018; Duan and Lu 2014; Crucitti et al. 2006), to take into account the change in travel time induced by the addition of new transport lines. It quantifies how efficiently information (or any other kind of flow) is exchanged over the network.

When the network is augmented by adding edges and vertices, a higher value of *AE* with respect to the original configuration denotes an improvement of the network performances in terms of a reduced average length of the shortest paths.

$$AE = \frac{1}{|V|(|V|-1)} \sum_{\substack{u,v \in V \times V \\ u \neq v}} \frac{1}{l_{uv}^{sp}} \tag{3}$$

where $l_{uv}^{sp}$ the length of the shortest path going from $u$ to $v$.

### *Local metrics*

To describe network performances at local scale, the edge betweenness centrality (*EBC*) (Eq. 4) (Freeman 1979) is among the preferred ones in the transport field and is largely used to identify bottlenecks of the traffic network. This metric characterizes the

importance of an edge as the number of times the edge is crossed by a shortest path. Although an edge with a high *EBC* might be considered as vulnerable in terms of resilience, it also means that the edge is very attractive and important to sustain flow in the graph, being crossed by a high number of shortest paths. Another widely used metric to assess the network performance at local scale is the node closeness centrality (*NCC*) (Freeman 1979) (Eq. 5), which quantifies how a given node $u$ is far from all the other ones by means of the sum of the reciprocal of the length of the shortest paths. As for the *AE*, the higher the *NCC*, the shorter the shortest paths. A node with a high *NCC* is in a short range from the rest of the network. The presented local metrics are used both on road network analysis and public transport ones (Crucitti et al. 2006; Berche et al. 2009; Chan et al. 2015).

$$EBC_e = \sum_{\substack{u,v \in V \times V \\ u \neq v}} \frac{\sigma_{uv}(e)}{\sigma_{uv}} \tag{4}$$

$$NCC_u = \sum_{\substack{v \in V_u \\ u \neq v}} \frac{1}{l_{vu}^{sp}} \tag{5}$$

where $\sigma_{uv}$ the number of shortest path joining nodes $u$ and $v$ in the graph and $\sigma_{uv}(e)$ the number of shortest path joining $u$ to $v$ crossing the edge $e$, $V_u$ is the set of nodes reaching from u, $|V_u|$ its cardinality and $l_{vu}^{sp}$ is the length of the shortest path going from the nodes $v$ to $u$ in the graph.

In the context of graph augmentation and centrality improvement, Bergamini et al. (2018) and Angelo et al. (2016) suggest to maximize *EBC* through an optimization problem by creating a limited set of edges. Crescenzi et al. (2016) consider a similar optimization problem by quantifying how much a node can increase its *NCC* by improving the reachability of the node via a reduction of the lengths of the shortest paths linking the node to the rest of the network, thus implyying a *NCC* increase. However, it is worth to mention that these approaches are extremely time consuming and therefore hardly apply to the settings of our study that focus on large metropolitan areas.

#### *Demand-aware metrics*

As reported in multiple studies from the transportation domain related to the quantification of performance and vulnerabilities of mobility networks, it appears crucial to include temporal and travel demand considerations when computing complex network metrics on transportation graphs. Several works deal with traffic volume in resilience assessment and in centrality metrics computation (Altshuler et al. 2011, Puzis et al. 2013, Leung et al. 2011). This is a fundamental aspect for resilience quantification due to the existence of correlation between centrality metrics and traffic flow, a subject that we also explored in our previous work (Henry et al. 2019a). For instance, in Kazerani and Winter (2009), the authors suggest to use data on travel demand to weight shortest paths in the computation of centrality metrics. Similarly, in Gauthier et al. (2018), the consideration of travel time data in shortest-path based centrality metric is proposed as a way

to merge both topology and traffic-related characteristics for transport network robustness analysis.

Based on such previous works, we consider travel demand in the computation of node degree centrality, by defining its demand-aware adaptation *DANDC* (Eq. 6). Similarly, $\langle DANDC \rangle$ (Eq. 7) represents the demand-aware network density.

$$DANDC_u = \delta_u.(|E_{uv}| + |E_{vu}|) \tag{6}$$

$$\langle DANDC \rangle = \sum_{u \in V} \frac{DANDC_u}{|V|} \tag{7}$$

where $\delta_u$ is the travel demand departing from and arriving to node $u$, with:

$$\delta_u = \sum_{v \in V_u} \alpha_{uv} + \alpha_{vu} \tag{8}$$

In the definition of the metrics above, rather than only considering the number of connected edges, we also account for the number of travelers departing from and arriving to the generic node $u$. In that sense, the $\alpha_{uv}$ coefficients ($\alpha_{vu}$, respectively) represent the part of the total travel demand, related to both private cars' and public transportation's users, going from area $u$ to area $v$ (from $v$ to $u$, respectively). More specifically, we consider that a path whose origin and destination belong to the road network only serves road users' demand. Otherwise, we consider that the demand served by the path is the sum of two contributions, i.e., the road part and the public transport one. In this work, we make the assumption that by augmenting and improving the public transport network offer, the latter can become more competitive and thus attractive for users who normally choose private vehicles for their travels. An improved and more attractive public transport system also improves traffic conditions by relieving the pressure on the roads.

Concerning the average efficiency metric, we take into account travel demand by weighting the efficiency of each path by using the same $\alpha_{uv}$ factor describing the part of the total travel demand it serves. The larger the demand associated to a specific pairs of nodes ($u$, $v$), the more such path will contribute to the average efficiency. With such formula modifications, both travel time and travel demand data will have an impact on the computation of the average efficiency, as from Eq. 9, i.e., shortest paths serving larger parts of the travel demand will therefore have a stronger impact on network efficiency.

$$DAAE = \frac{1}{|V|(|V|-1)} \sum_{\substack{u,v \in V \times V \\ u \neq v}} \alpha_{uv}.\frac{1}{l_{uv}^{sp}} \tag{9}$$

By modifying the definition of the *EBC* to consider the demand, Altshuler et al. (2011) notice a different distribution of *EBC* with respect to the unweighted classical BC definition, better correlated to typical flow information. Following similar approaches, Zhao et al. (2017) suggest that modified definitions of network centrality metrics that take into account both geometric properties and traffic information of the road network could lead to an improved traffic flow analysis and accurate predictions of flows at different

levels. We found similar conclusions in our previous article Henry et al. (2019a) where we proved the exisence of a spatio-temporal correlation between the demand-aware *EBC* (*DAEBC*) (Eq. 10) and the traffic flow. With such *DAEBC* formulation, the importance of an edge with respect to the network depends on the number of shortest paths crossing the edge, but also on the part of demand that travels through the edge for a specific pair of origin/destination nodes. A public transport edge with a high *DAEBC* means that the transport line is interesting with respect to the travel time, considered in the shortest path computation, and will be largely chosen by the travelers.

$$DAEBC_{uv} = \sum_{\substack{u,v \in V \times V \\ u \neq v}} \alpha_{uv}.\frac{\sigma_{uv}(e)}{\sigma_{uv}} \tag{10}$$

$$DANCC_{u} = \sum_{\substack{v \in V_u \\ a_1 \neq v}} \alpha_{vu}.\frac{1}{l^{sp}_{vu}} \tag{11}$$

Regarding the demand-aware *NCC* (*DANCC*), we assume that the importance of a node depends on the demand it attracts. With such definition (Eq. 11) the quicker the node is reachable from all the other ones in the network, in terms of travel time on which the shortest path calculation is based, and the higher the demand that is associated to paths including the node as a destination, the greater the *DANCC*.

#### Related works on graph augmentation and complex networks modelling

The methodology falls within the network design and the graph augmentation fields. In the context of graph augmentation and centrality improvement, Bergamini et al. (2018) and Angelo et al. (2016) suggest to maximize the Node Betweenness Centrality (*NBC*) measure through an optimization problem by creating a limited set of edges. Crescenzi et al. (2016) consider a similar optimization problem by quantifying how much a node can increase its Node Closeness Centrality (*NCC*) measure with a graph-augmentation-based approach. However, it is worth to mention that these solutions are extremely time consuming and therefore hardly apply to the settings of our study that focus on large metropolitan areas with a multimodal transport network.

Regarding the complex networks context, Aleta et al. (2017) propose a model able to easily assess network improvements as the addition of new lines. By modeling the public transport network of different cities as a multiplex networks, the authors characterize the network properties using the overlapping degree, equal to the sum of the nodes degree, and the transport mode's layer inter-dependency. The authors also consider traffic conditions in the multi-layer graph by weighting the intra-layer edges with the corresponding travel time and sets the total walking time and the waiting one to the inter-layer edges. Due to the lack of passenger flow data, the authors ignore such level of details. They prove the utility of centrality measures in a multi-layer graph to capture the impact of a specific and unique line addition. Nonetheless, such approach is not adequate for a quasi real-time context and is not practicable for a large set of transport lines, again due to the high computational time.

The novelty of our approach consists in a fully fledged methodology that leverages traditional resilience metrics to quantify the impact of augmenting an existing transport network with the addition of one or more additional transport-mode lines. Moreover, our approach investigates the usage of a multi-layer network model to simplify the representation of the multi-modal transport network and allow quickly computing several global and local metrics.

## The REINFORCE methodology

The REINFORCE methodology aims at prioritizing the construction of multiple, already designed/routed transport lines or modes, as well as ranking alternatives for deploying an emergency transport service, such as a dynamic ensemble of bus lines explicitly designed for reactively managing an unforeseen hazardous event that might disrupt the transport network. This prioritisation is based on the quantification of the performance improvement that derives from the addition of the considered transport lines. To that purpose, REINFORCE adopts a multi-layer graph modelling of the urban multi-modal transport network and a set of global and local metrics to quantify the performance improvement.

Since we aim at applying REINFORCE to large-scale transport networks, which represents an objective not compatible with a quick computation of certain graph metrics such as *EBC*, we adopt an approach based on graph simplification. By relying on multiple fine-grained networks as input, each representing a specific transport mode (e.g., road network, bus lines, subway lines, etc.) of the analyzed transport system,[1] our solution produces a macroscopic graph, which we call *macro-graph* in the following, that constitutes an aggregate, simplified and unified abstraction of the whole multi-modal urban mobility system.

Each node of the macro-graph is considered to be located at the centroid $c_i$ of an area $A_i \in \mathcal{A}$, whose spatial extent can be covered on foot. After the creation of the macro-nodes, REINFORCE creates a layer $l$ for each transport mode and an inter-layer edge $e^l \in E_l$ between any two areas $(A_i, A_j)$ if at least one edge exists among any pair $(v_i^l, v_j^l)$ of nodes from the initial fine-grained graph representation of transport mode $l$, where $v_i^l$ is selected from the set of nodes belonging to area $A_i$ and $v_j^l$ is selected from those related to area $A_j$, in order to preserve an accurate connectivity in the multi-layer simplified abstraction.

Based on this approach, we consider two cases, both presented In Fig. 1a. In the first case, no direct edge joining area $A_1$ to area $A_3$ exists. Thus, no edge is created in the macro-graph between these two areas for the specific analyzed mode. In the second case, a connection exists because of the presence of the direct edge connecting the blue nodes in areas $A_1$ and $A_3$ from the fine-grained underlying graph. For each transport mode we follow the same approach to simplify the corresponding fine-grained graph.

[1] The fine-grained inputs of our methodology are simple directed graphs modelling each transport mode individually, at the finest available level of details and spatial resolution. More specifically, for road networks, we use in our experiments a graph representing road intersections with nodes and road segments with edges. For tramway lines, the fine-grained graph includes a node for each tramway stop on a given tramway line and a directed edge for each line segment connecting pairs of bus stops belonging to the same line. Finally, for the subway network, the graph includes a node for each metro station on a given subway line and a directed edge for each subway segment of a given line connecting two metro stations.

Our final macro-graph is composed of three layers corresponding to each of the considered transport modes: road, tramway and subway.

Concerning inter-layer connectivity, the basic idea is to model inter-modal transitions that can be available to travellers in a given area of the city. Such transitions are represented in the macro-graph via inter-layer edges that are created between replicas of the centroid node corresponding to the considered area. These inter-layers edges can only exist if at least two transport modes are present in the area, and, in such a case, the node corresponding to the area is duplicated and the two replicas of the area node are connected via a weighted bi-directional inter-layer edge. The weights of the inter-layer edges are determined based on the specific features of the transport mode transitions that are possible in each specific area. Specifically, we define inter-layer weights in terms of *the average area walking time*, i.e., the mean pair-wise walking travel time computed according to a walking speed of 1.5 m/s. The pair-wise walking travel times within an area are computed between each road intersection and public transport stops of the given area, as well as between the transit stops belonging to the subway or the tramway networks. The inter-layer weight in an area providing access to multiple transport modes thus depends on the specific features of the area and, particularly, on the density of the transport network inside it: the proposed procedure to define an inter-layer weight allows taking into account the (average) walking time necessary to perform a modal shift inside each area. The values of the weight are comprised between 3.8 and 8.7 min for modal shifts between the road network to a public transport mode, and between 0.0 and 10.1 min for modal shifts on the public transit system of the city (Fig. 2). In addition, concerning modal changes related to the private vehicle mode, we penalize more the inter-layer edges within areas that do not include dedicated car parks for mode change to transit (i.e., park-and-ride stations). Specifically, we increase the weight of 3.5 min for the inter-layer edges related to the road-transit, when there is no park-and-ride station in the associated area in order to model the delay necessary to find a parking space. As observed by Lefauconnier (2005), in the city of Lyon, people spent in average 11.8 min per day to find a car park and 3.3 displacements are realized in average per day.[2]

Concerning the weights of the intra-layer edges, we weight each edge of the macro-graph by means of some traffic indicators, depending on the studied metric, under the hypothesis of free-flow conditions. Consequently, edge weights are considered to be static and the impact of traffic dynamics as well as users' route choices are not taken into account in this study. This could represent a limitation of the present study which is currently unable to address complex (dynamic) scenarios (e.g., Braess's paradox (Braess et al. 2005)). Concerning the metrics based on shortest path computation (*AE*, *EBC* and *NCC*), we compute, for all the transport mode network layers, the weight associated to the edge connecting any two centroids $c_i$ and $c_j$ of areas $A_i$ and $A_j$ by averaging the length of the shortest paths computed over the free-flow weighted sub-graph $G[A_i, A_j]$ induced on the original, fine-grained modal graph by the subset of nodes included in both areas $A_i$ and $A_j$ (Fig. 1a), i.e.:

[2] http://www.sytral.fr/472-sur-lyon-villeurbanne.htm.

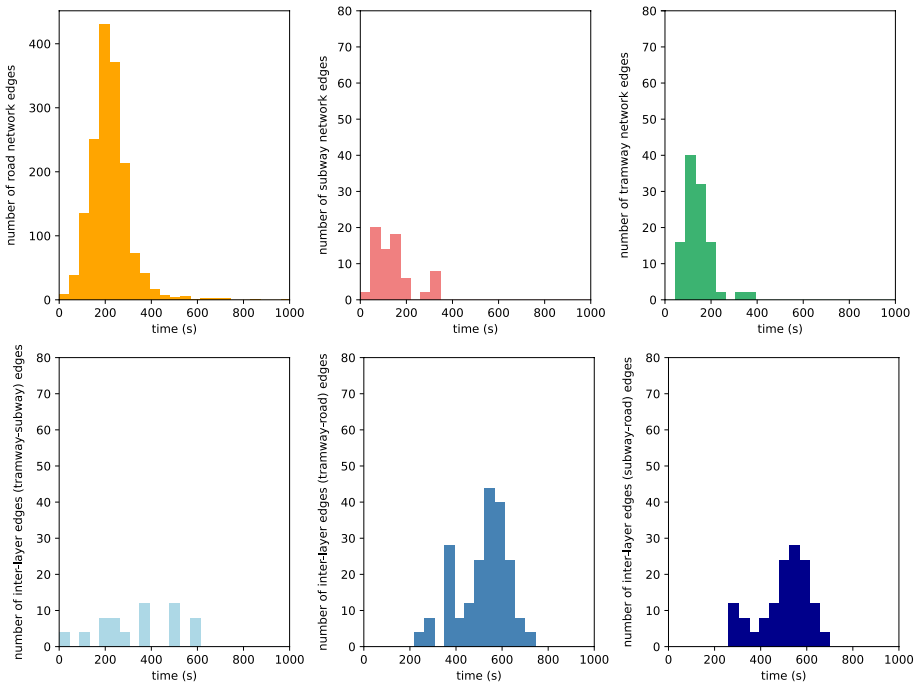


**Fig. 2** Intra-layer edge weight distributions for the road network (orange), the subway network (pink) and the tramway network (green), and inter-layer edges weight distribution between public transport system modes (light blue), between the road network and the tramway network (blue), between the road network and the tramway network (dark blue)

$$\forall A_i, A_j \in \mathcal{A} \times \mathcal{A}, \quad \text{if } P_{A_iA_j} \neq \emptyset, \quad w^{mode}_{c_ic_j} = \frac{1}{|P_{A_iA_j}|} \sum_{p \in P_{A_iA_j}} f(p) \tag{12}$$

where $\mathcal{A}$ is the set of hexagon areas, $c_k$ the centroid of the area $A_k$, $P_{A_iA_j}$ the set of the shortest paths of the sub-graph $G[A_i, A_j]$, $|P_{A_iA_j}|$ the cardinality of the set $P_{A_iA_j}$ and $p \mapsto f(p)$ the function which computes the free flow travel time of path $p$. We assume the subway network free flow speed to be about 40 km/h, and the tramway one to be about 30 km/h (Hitge and Vanderschuren 2015).

In order to take into account users' bounded rationality (Henry et al. 2019b) in the computation of the shortest paths, the weights of the macro-graph have been discretized as follows. Firstly, for each transport mode, the weight range has been divided into intervals whose width increases as the weight increases at rate $\gamma$ (set at 0.75 in our study), i.e.:

$$\forall m \in T_m, I^m_i(\gamma) = [min_m(1+\gamma)^{i-1}; min_m(1+\gamma)^i] \tag{13}$$

where $T_m$ is the set of transport mode (car, tramway, subway), $I^m_i$ is the $i$th interval considered for mode $m$, $min_m$ is the minimum weight observed for edges of mode $m$, and $\gamma$ is the rate at which the width of the intervals increases. Secondly, for each edge of weight $w$ belonging to mode $m$, $w$ is discretized by taking the integer value closest to the average of the weights falling in the interval of mode $m$.

Once the weights have been assigned to the macro-graph, shortest paths can be computed between macro-graph nodes (area centroids) to calculate the metrics in their

traditional definition (*AE*, *NDC*, *NCC* and *EBC*) or in their demand-aware adaptation (*DAAE*, *DANDC*, *DANCC* and *DAEBC*).

Lastly, concerning our main objective of prioritizing the construction of multiple transport lines, we select the best combinations by computing the selected network performance metrics for each possible scenario of joint construction. As reported in Fig. 1b, we first create the set $S$ of all the $\binom{N}{k}$ considered scenarios, where $N$ is the total number of new transport lines designed to be built and $k \leq N$ is the number of lines that we allow to be jointly constructed. This number $k$ could be determined by considering budget constraints, roadworks space consuming, the available labor, etc. Because of the large number of combinations, we aim at first computing, for all scenarios, the global indicators $AE$ and $\langle NDC \rangle$ ("Global metrics" section) atop the newly computed macro-graph that includes any pre-existing transport line or mode, plus all the new lines to be built for a given scenario $s$, and quantify the global impact of the scenario. The computation of these indicators is not time-consuming and thus respects our desire to propose a quick-to-compute methodology. After computing $AE$ and $\langle NDC \rangle$ on the graph induced by each scenario $s$, it is possible to sort scenarios with respect to a given metric $m \in \{AE, \langle NDC \rangle\}$, and compute the ranking $rank_m(s)$ of $s$ among all considered scenarios, with respect to the given metric $m$ (*e.g.,* the scenario with highest $AE$, will receive $rank_{AE}$ equal to 1, while the one with lowest $AE$ will receive $rank_{AE}$ equal to $\binom{N}{k}$). Thus, we are able to select the most interesting scenario via the objective function: $argmin_{s \in S}(rank_{AE}(s) + rank_{\langle NDC \rangle}(s))$. In addition to the most interesting scenario, i.e., the one that minimizes the aforementioned objective function, we also consider the second- and third-best scenarios for our local analysis. The global characterization of the scenarios is crucial to reduce the number of scenarios to be analyzed at local scale. Then, we focus on the local indicators (*EBC* and *NCC*) ("Local metrics" section) for the reduced set of three best scenarios because of the complexity in computing such indicators. Nonetheless, such indicators are essential to observe the spatial impact of adding new transport lines. The global characterization of the scenario is crucial to reduce the number of scenarios to be analyzed at local scale.

## Case study

We apply the REINFORCE methodology on the transportation network of Lyon, France (Fig. 3a) and some peripheral adjacent towns. The reasons of this choice are both the availability of data and our knowledge of the city. The public transport network of Lyon is composed of 7 tramway lines (progressively numbered from 0 to 6 as reported in Fig. 3e) and 5 subway lines (labelled with letters A, B, C, D, E, F1, F2, as from Fig. 3d). Because REINFORCE aims at prioritizing the construction of a transport mode, we assume that the public transport (tramway (Fig. 3e) and subway (Fig. 3d)) networks are not constructed. Lyon's transport network is thus supposed to be only composed by the road network (Fig. 3c).

Such an assumption is motivated by the desire to evaluate the applicability of our approach on a large network. In our future works, we aim at (1) using this approach to plan the construction of non-existing transport lines or for the post-disaster reconstruction of transport lines; (2) using this approach for emergency planning of temporary transport lines for resilience enhancement and short-term disaster response.

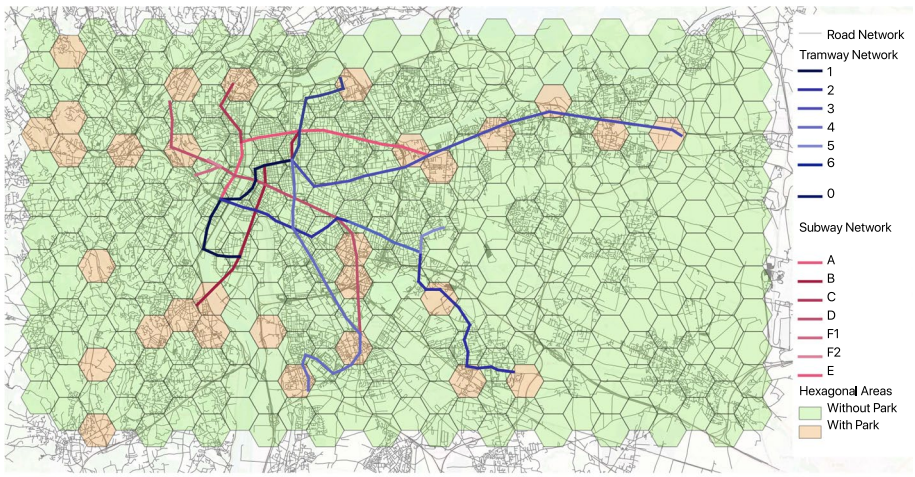


**(a)** Real Transport network with the hexagon areas used for the macro-graph construction. The orange areas are those where a car park dedicated for modal change exists.

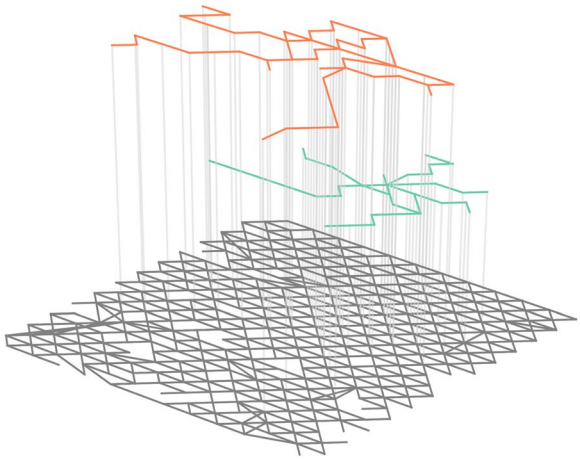

**(b)** Multilayer Transport network with the road network **(c)**, the subway one **(d)** and the tramway one **(e)** with the inter-layer edges in light grey.

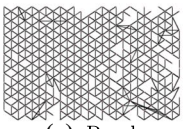

**(c)** Road

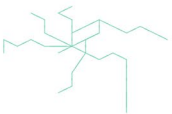

**(d)** Subway

**(e)** Tramway

**Fig. 3** The real transport network of Lyon and its hexagon tessellation (**a**). The simplified macro-graph (**b**) when all public transport lines are constructed, with its road network (**c**), subway network (**d**) and tramway network (**e**) layers

Regarding the second point, we succinctly explore such application of REINFORCE by considering the prioritization of line construction during a special event, Lyon's "Festival of Lights", that takes place yearly in the city attracting a very large amount of tourists and drastically changing the travel demand.

To model the simplified multi-layer macro-graph we use 324 hexagon area with a maximal length of 1km, which was found to be a good compromise between computing time and graph accuracy. The resulting hexagon area size respects a walkable distance in accordance with our previously described graph simplification method, where transport modes link the centroids of the different areas. Although our study focuses on the spatial area delimited by the extent of the subway and tramway

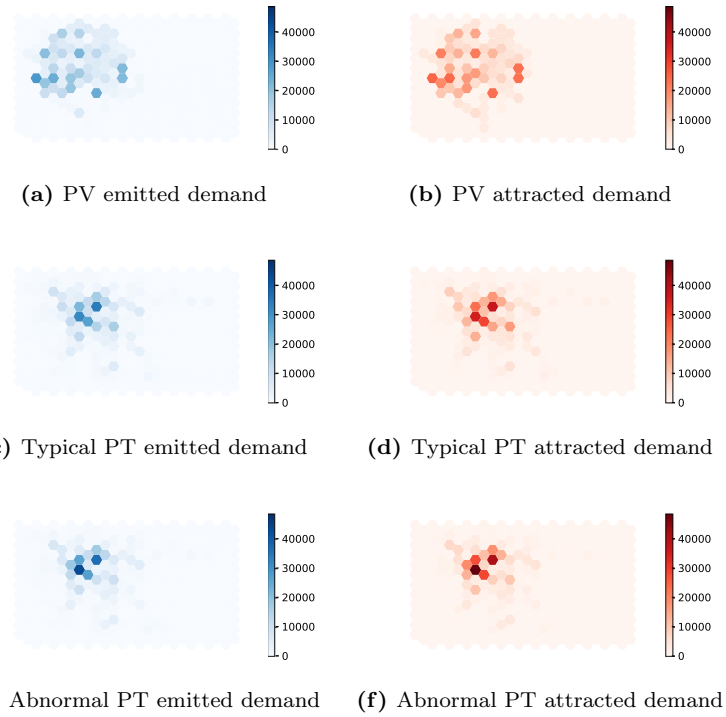


**Fig. 4** Typical private vehicles' (PV) travel demand emitted (blue) (**a**) and attracted (red) (**b**) by the areas. Typical emitted (blue) (**c**) attracted (red) (**d**) public transport (PT) travel demand, and abnormal emitted (blue) (**e**) attracted (red) (**f**) public transport travel demand

networks, to mitigate the border effect on the centrality metrics (Porta et al. 2006) computed on the macro-graph, we also consider a buffer area around the two studied public transport networks that only includes portions of the road network. This permits to include potential road paths joining pairs of areas more efficiently than the public transports in the computation of the metrics.

The scenario including all the public transport lines is the optimal one. The corresponding multi-layer graph is composed of 407 nodes and 1 986 edges of which 1 606 belong to the road network (Fig. 3c), 70 to the subway one (Fig. 3d) and 110 to the tramway one (Fig. 3e). 200 edges permit to transit from a transport mode to another one at the centroid of the areas. For a clearer visualization we use an undirected representation of the graphs in Fig. 3. Longer road edges in Fig. 3c represent highways or peripheral roads which directly join farther areas of the city.

To infer travel demand coefficients, we use two datasets (Fig. 4). The first one provides private vehicles' demand (Fig. 4a, b) whereas the second ones are related to the public transport demand under normal condition (Fig. 4c, d) and during a specific event (Fig. 4e, f). For both datasets travel demand is provided at the level of the finer-grained graphs used as inputs for the construction of the macro-graph. Therefore, we have adapted such data to our simplified representation: the demand associated to a given pair of hexagon areas $(A_i, A_j)$ has been obtained by summing up the demands related to all pairs of nodes $(v_k, v_l)$ from the initial finer-grained graph where $v_k \in A_i$ and $v_l \in A_j$.

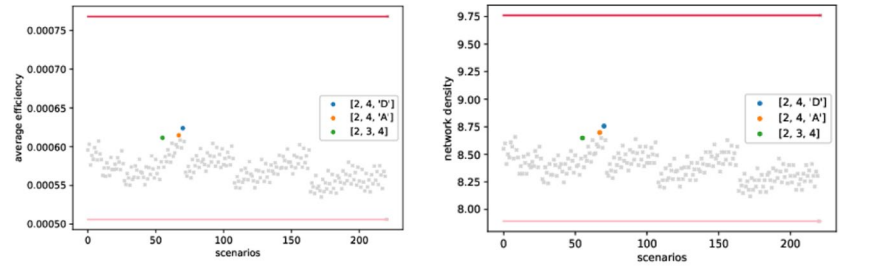


**(a)** Average Efficiency **(b)** Density

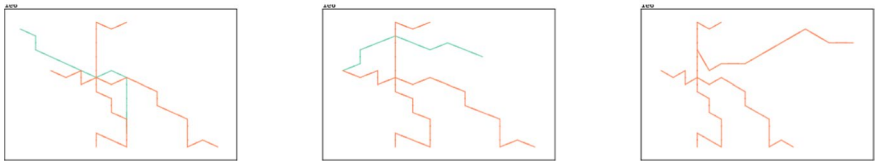

**(c)** Network - lines 2, 4, D **(d)** Network - lines 2, 4, A **(e)** Network - lines 2, 3, 4

**Fig. 5** Global indicators *AE* and $\langle NDC \rangle$ for all the scenarios consisting in adding three new transport mode lines

To explore the ability of REINFORCE to capture traffic conditions, we analyze the impact of a large increase of the public transport demand over the selected lines. To this purpose, we use the recorded public transport demand during the Festival of Lights ("Fête des Lumières") in Lyon that attracted 1.8 billion people in 2017.

## Results

In our experiments, we assume that 3 out of 12 lines are built simultaneously, which corresponds to $x = \binom{12}{3} = 220$ scenarios. As explained in the REINFORCE methodology description, we first compute the global indicators for the 220 line combinations before analyzing the impact of a reduced set of scenarios at local scale. The computational time related to the first step does not exceed 4 min.

### Traditional metrics

In this section, we study the impact of adding new public transport lines by quantifying their impact through traditional metrics that do not take demand into account. We thus compute the $\langle NDC \rangle$ and the *AE* to select the three best scenarios at global scale and then analyze the local impact by computing the *NCC* and the *EBC*.

#### *Global analysis*

In Fig. 5, we plot the values of *AE* (Fig. 5a) and $\langle NDC \rangle$ (Fig. 5b) for all the 220 scenarios corresponding to the construction of three public transport lines. We also plot the values of these metrics for the two reference scenarios where: (i) there is no public transport lines (light pink bottom line in Fig. 5a, b); (ii) all the 5 subway and 7 tramway lines (dark pink line in Fig. 5a, b) are considered as constructed. Higher *AE* values indicate that the addition of the transport lines significantly improves the efficiency of the network with respect to the reference scenario with no public transport line, by reducing on average the travel time of the shortest paths. In other words, it is quicker to reach

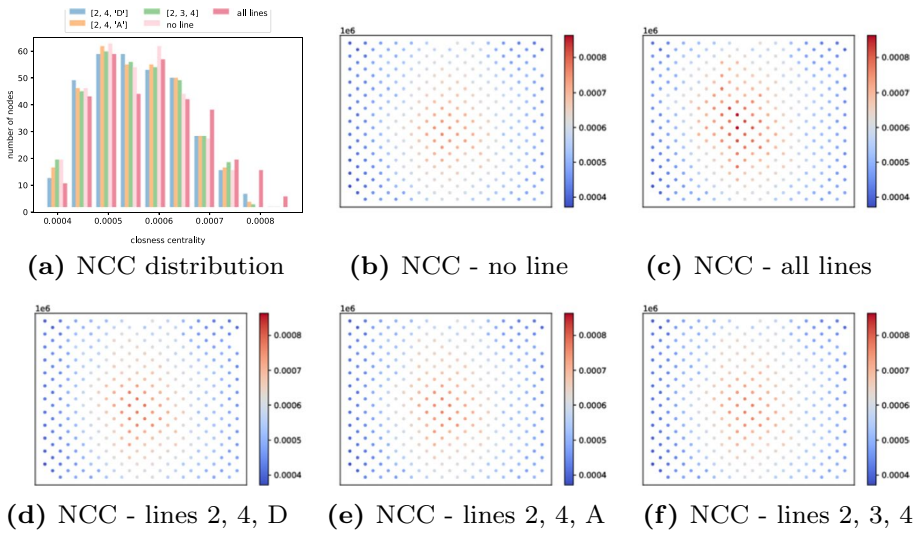


**(a)** NCC distribution **(b)** NCC - no line **(c)** NCC - all lines

**(d)** NCC - lines 2, 4, D **(e)** NCC - lines 2, 4, A **(f)** NCC - lines 2, 3, 4

**Fig. 6** Histogram of node closeness centrality and its spatial distribution in the studied scenario

the different areas of the graph thanks to the presence of the additional public transport (subway and tramway) lines.

An increase of $\langle NDC \rangle$ corresponds to the addition of new connections between the different nodes of the network. The original network (only including roads) is almost a 12-regular graph. Each area is connected to its neighbors by in-going and out-going edges. Therefore, an increase of the density is the result of the creation of alternative paths using public transport modes.

Scenarios are sorted by computing a score which is equal to the sum of their rank for both global metrics ($AE$ and $\langle NDC \rangle$), as detailed in "The REINFORCE methodology" section. The scenarios corresponding to smaller scores indicate that both $AE$ and $\langle NDC \rangle$ are higher. We select the three scenarios with the smallest scores. Then, such scenarios are analyzed at local scale to provide a description of the geographical impact of the construction of the selected lines. Due to computational limitations, it is essential to reduce the set of selected scenarios before starting the local analysis.

In free flow conditions and without considering the travel demand, the three best combinations of lines to be built, according to the global indicators, are the joint creation of lines {2, 4, D} (Fig. 5c), {2, 4, A} (Fig. 5d) and {2, 3, 4} (Fig. 5e).

### Local analysis

Figure 6 summarizes the impact on $NCC$ (Eq. 5) induced by the three selected construction scenarios and the two reference ones. The improvement on the network efficiency induced by the public transport lines construction is noticeable in the reported plot of the distribution of the $NCC$ metric (Fig. 6a). The $NCC$ distribution shifting to higher values (with respect to the baseline scenario with no public transport) confirms an increase of the number of nodes with high $NCC$, meaning that macro-graph nodes are globally closer to each other, generally improving the characteristics of the transport network in terms of shortest paths: it is easier and quicker to reach an area from all the other ones.

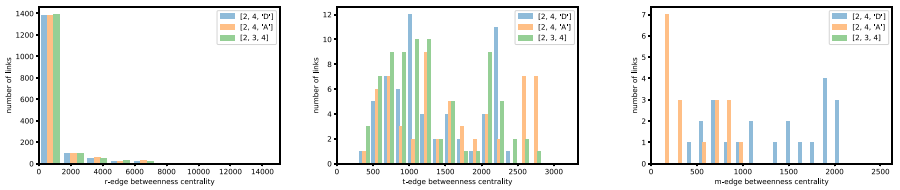


**(a)** EBC - road network **(b)** EBC - tramway network **(c)** EBC - subway network

**Fig. 7** Histogram per transport mode of the *EBC* in the studied scenarios

The light pink scenario, with no public transport line, has the leftmost skewed distribution, whereas the dark pink scenario, where all the public transport lines are constructed, has the rightmost one. Both observations are in accordance with Fig. 6b, where the vast majority of nodes exhibits lower *NCC* values with respect to Fig. 6c, related to all lines built, which, unsurprisingly, denotes significantly higher values of *NCC*, especially in city center areas. Concerning the three selected construction scenarios, we observe a higher number of nodes with high *NCC* in scenario {2, 4, D} (see Fig. 5c) as denoted in Fig. 6a. For the two remaining scenarios, the construction of lines {2, 3, 4} (Fig. 5e) appears as the least attractive in terms of *NCC*. Indeed, the distribution of *NCC* is more shifted to lower values than scenario {2, 4, A}(Fig. 5d).

Figure 7 presents the distribution of the *EBC* (Eq. 4) per transport mode in each of the studied scenario. The more the *EBC* distribution is shifted to the right, the more links tend to be crossed by a high fraction of shortest paths per pairs of origin/destinations. Independently of the scenario, we observe that the majority of road network edges have very low values of *EBC* (Fig. 7a). This means that most of these edges are crossed by a small fraction of shortest paths or none at all.

This trend is similar in all of the three selected scenarios concerning road network edges. However, concerning the tramway lines (Fig. 5e), we observe in scenario {2, 3, 4} a larger set of edges with *EBC* close to 0 than in the two other scenarios (Fig. 7b). Indeed, 17 edges have a quasi-null *EBC* in this scenario, against 13 in scenario {2, 4, A} (Fig. 5d) and 12 for the scenario {2, 4, D} (Fig. 5c). A similar trend can be observed for the subway network (Fig. 7c). Whereas in scenario {2, 4, A} (Fig. 5d) 12 edges of the A-line are almost never crossed by shortest paths, almost all D-line edges in scenario {2, 4, D} make the transport network more efficient by being crossed by a large number of shortest paths.

### Demand-aware metrics

In this section, we describe the results obtained in our experimentation when using both global and local metrics in their demand-aware adaptation described in "Demand-aware metrics" section and introduced to account for the impact that travel demand might have in the construction of new transport lines. By using such metrics, the importance of a line depends not only on the amount of travel time it permits to save, but also on the amount of travel demand it can serve. When a line is not present in a given construction scenario, we adopt the simplifying assumption to remove the associated demand, without reassigning it over other existing lines.

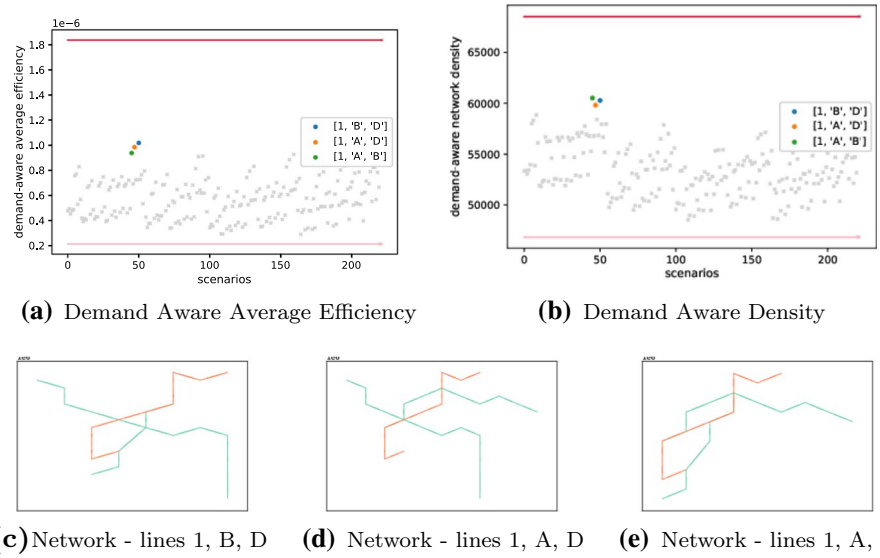


**(a)** Demand Aware Average Efficiency **(b)** Demand Aware Density

**(c)** Network - lines 1, B, D **(d)** Network - lines 1, A, D **(e)** Network - lines 1, A, B

**Fig. 8** Global indicators *DAAE* and ⟨*DANDC*⟩ for all the scenarios consisting in adding three new transport mode lines

By this approach, a public transport line is considered more attractive if it allows to connect areas more rapidly than the road network and the associated demand is significant.

### *Global analysis*

Following the same methodology adopted for demand-unaware metrics (see "Global analysis" section), we notice some differences in relation to the previously selected three best scenarios, obtained when using global metrics. Indeed, whereas with demand-agnostic metrics we found {2, 4, D} (Fig. 5c), {2, 4, A} (Fig. 5d) and {2, 3, 4} (Fig. 5e) as the three best scenarios, when sorting all the possible scenarios based on the ranks of demand-aware global metrics (*DAAE* and ⟨*DANDC*⟩), we find lines {1, B, D} (Fig. 8c), {1, A, D} (Fig. 8d) and {1, A, B} (Fig. 8e) to be the three best alternatives. This result appears to be in accordance with the emitted (Fig. 4c) and the attracted (Fig. 4d) public transport travel demand. In fact, the westernmost darker-blue area in Fig. 4c (corresponding to the westernmost darker-red one in Fig. 4d) presents the highest emitted (resp. attracted) demand of the city and it is reachable with the A and the D subway lines, as well as via the 1 tramway line. Likewise, concerning the northernmost darker-blue (Fig. 4c) and darker-red (Fig. 4d) areas, lines 1, 4, A and 3 allow to reach such high-demand zones of the city. Regarding the southernmost darker-blue and darker-red areas, the B-line serves them to reach the north of the network by also crossing the darker-blue and darker-red central zone (Fig. 4c, d) which corresponds to an important transit hub of the city of Lyon. It appears therefore consistent to observe the aforementioned scenarios (i.e., {1, B, D}, {1, A, D} and {1, A, B}) as the best results when using demand-aware global metrics with the REINFORCE methodology (Fig. 3).

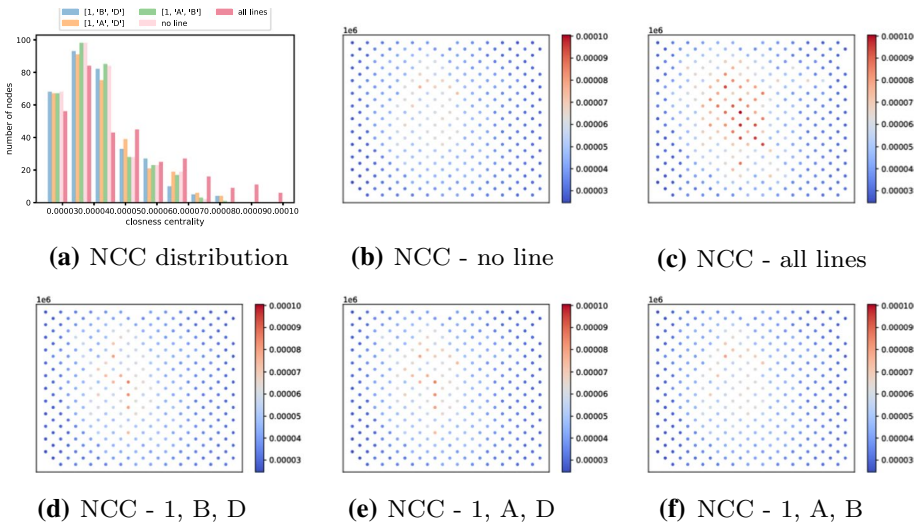


**(a)** NCC distribution **(b)** NCC - no line **(c)** NCC - all lines

**(d)** NCC - 1, B, D **(e)** NCC - 1, A, D **(f)** NCC - 1, A, B

**Fig. 9** Histogram of *DANCC* and its spatial distribution in the studied scenarios

### *Local analysis*

When considering demand-aware local metrics, we first notice, for our baseline scenarios, that the *DANCC* distribution (Fig. 9b) with no public transport line presents a very similar behaviour with respect to the *NCC* one (Fig. 6b), although the values change due to the consideration of the demand in the metric computation. When considering the addition of all public transport lines, the distribution is shifted to the right, meaning that more nodes have higher values of *DANCC*. Similar conclusions can be drawn for the three best selected scenarios with this demand-aware local metric (*DANCC*). The accessibility of some nodes is improved as demonstrated by the reduction of the number of nodes with low values of *DANCC* with respect to the reference scenario without any public transport line. As for the results obtained with the demand-unaware metric (*NCC*) (Fig. 6), the addition of public transport lines improves the reachability of some areas in the transport network of Lyon. The two first scenarios {1, B, D} (Fig. 9f) and {1, A, D} (Fig. 9g) improve the reachability of the center-southern part of the network via the construction of the D-line, whereas concerning scenario {1, A, B} (Fig. 9h), an improvement can be identified for the center-northern part of the city. Nonetheless, we notice that the improvement induced by this scenario is mild compared to the other two, as also highlight by the distribution of the metric reported in Fig. 9a (the histogram related to scenario {1, A, B} is slightly skewed to the left compared to the other two).

Concerning the *DAEBC* distribution per transport mode (Fig. 10), we notice a major change with respect to our analysis based on traditional demand-unaware *EBC*, due to our modification of the metric by including a demand-dependent multiplicative factor. For the road network (Fig. 10a) edges, the trend is similar in all scenarios: a large set of edges is crossed by a very small amount of shortest paths. Nonetheless, edges of both public transport networks (tramway and subway) present lower *DAEBC* values than the *EBC*. This is especially true with the tramway network, which appears, via the 1-line, in all the selected scenarios with similar trend. Whereas 11 edges of the 1-line have very marginal influence on the network performance by presenting a *DAEBC* close to 0, 1

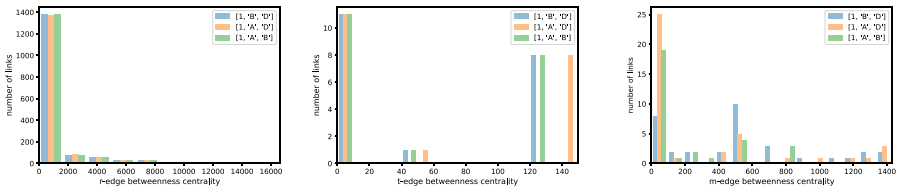


**(a)** EBC - road network **(b)** EBC - tramway network **(c)** EBC - subway network

**Fig. 10** Histogram per transport mode of *DAEBC* in the studied scenarios

edge of this line still presents an interest, i.e., *DAEBC* significantly larger than 0, while 8 other edges of the 1-line are crossed by a much larger amount of shortest paths, i.e., *DAEBC* presents values significantly larger than 100. In particular, the second scenario, {1, A, D}, (Fig. 8d) presents even higher values of *DAEBC*. Indeed, the 8 most attractive edges of the 1-line present *DAEBC* values higher than 140, against values comprised between 120 and 130 for the 8 same edges in the two other scenarios. This means that the line is more used in the scenario {1, A, D} when the B-line is not built. Finally, concerning the subway network (Fig. 10c), only 7 edges have a non-zero *DAEBC* in scenario {1, B, D} (Fig. 8c) against 25 edges in scenario {1, A, D} and 18 edges in scenario {1, A, B}. The scenario {1, A, B} presents the less attractive distribution, by being more skewed to the left. The huge difference between the *EBC* and the *DAEBC* is due to the demand factor in the metric formulation (Eq. 10).

### Impact of a special event

In this last section, we analyze the impact of the 2017 Lyon's "Festival of Lights", a very popular event that attracted 1.8 billion of visitors that strongly solicited the transport network of the city. We use the specific public transport travel demand observed during these days rather than a typical one. The goal of this analysis is dual. Firstly, we aim at confirming the ability of our methodology to capture travel demand information for the prioritization of line construction scenarios. Secondly, we aim to show an example in which the methodology could be helpful to dynamically reconfigure the transport network. The idea is to compute, on-the-fly, the best combination of newly designed transport lines to be deployed in order to handle an exceptional situation that might significantly disrupt the quality of the transport offer of a city.

#### *Global analysis*

By considering the public transport travel demand recorded during the "Festival of Lights" in the computation of our demand-aware global indicators (*DAAE* and $\langle DANDC \rangle$) (Fig. 11a, b), the best three scenarios are the same as the one computed under normal demand conditions. However, the ranking of the three best scenarios change. Now the three scenarios selected through demand-aware global metrics are in the order: {1, A, D} (Fig. 8d), {1, A, B} (Fig. 8e) and {1, B, D} (Fig. 8c). In particular, in the presence of the selected special event, scenario {1, A, D} (Fig. 8d) becomes more interesting than the {1, B, D} one (Fig. 8c). This is legitimated by the fact that, during the "Festival of Lights" some subway stations covered by line A (e.g., Bellecour square, Hotel de Ville,

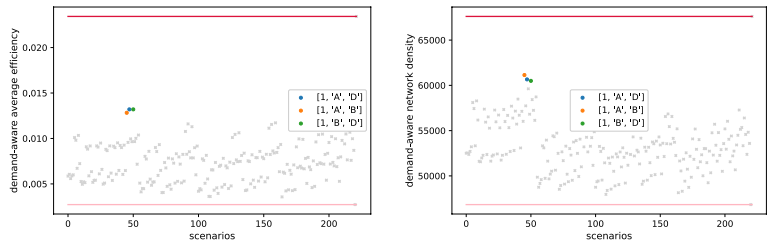


**(a)** Demand Aware Average Efficiency **(b)** Demand Aware Density

**Fig. 11** Global indicators *DAAE* and (*DANDC*) for all the scenarios consisting in adding three new transport mode lines during the "Festival of Lights"

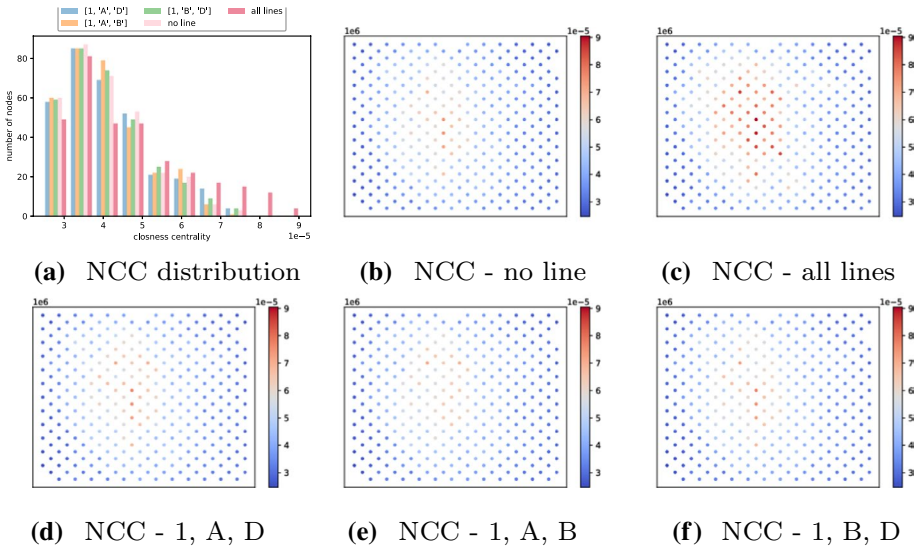


**(a)** NCC distribution **(b)** NCC - no line **(c)** NCC - all lines

**(d)** NCC - 1, A, D **(e)** NCC - 1, A, B **(f)** NCC - 1, B, D

**Fig. 12** Histogram of *DANCC* and its spatial distribution in the "Festival of Lights" scenario

Cordeliers) and line D (e.g., Bellecour square) are the most impacted by the event. In fact, these areas attract a larger than usual demand (Fig. 4e, f), especially due to visitors wanting to participate to light spectacles taking place at such city-center zones.

### *Local analysis*

The shape *DANCC* distribution (Fig. 12b) does not change significantly from the one observed with typical public transport demand (Fig. 9b), although the values are impacted by the change in the demand. Nonetheless, the spatial distribution of the metric over the areas is modified and this change is more visible when all the public transport lines are built. The *DANCC* of the two areas with the highest demand is high (Fig. 12c). In this case also, the D-line improves the reachability of the south of the network in scenarios {1, A, D} and {1, B, D}.

Concerning the analysis of the *DAEBC* metric, around 200 road-network edges presents an advantage in the multi-layer network performance by being crossed by a huge amount of shortest paths ($DAEBC > 2000$) (Fig. 13a). Moreover, the distribution of the *DAEBC* values for scenario {1, A, D} presents a slightly lower number of quasi-zero

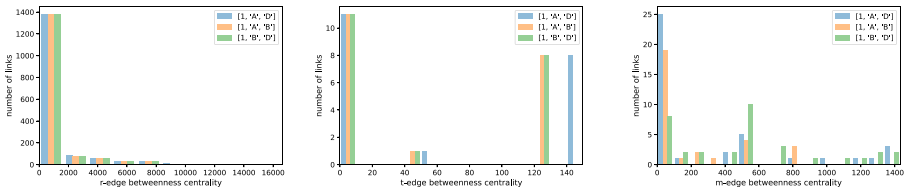


**(a)** EBC - road network **(b)** EBC - tramway network **(c)** EBC - subway network

**Fig. 13** Evolution per transport mode of *DAEBC* in the "Festival of Lights" scenario

*DAEBC* than the two other scenarios. A reduced number of shortest paths crosses tramway-network edges, due to the smaller demand along the 1-line compared to the demand along the subway lines (Fig. 13b). A small number of the tramway-network edges appears to be interested by a network performance improvement in relation to *DAEBC* and the scenario {1, A, D} still presents a small but better improvement compared to the two others scenarios by presenting edges crossed by a higher number of shortest paths and attracting a higher demand. Nonetheless, whatever the analyzed scenario, the 1-tramway line appears important and largely used. Finally, for the subway network (Fig. 13c), scenario {1, A, D} presents 25 quasi-zero *DAEBC* edges against 19 for scenario {1, A, B} and 8 for scenario {1, B, D}. In this last scenario, more edges are interesting in terms of transport network performance, according to the *DAEBC* distribution, which appears shifted to the right.

## Conclusion and future works

We proposed the REINFORCE methodology for quick augmentation of large multimodal transport networks, easily adaptable to any city for which the actual transport network offer is known, jointly with a plan of the new transport lines/modes to be built. The proposed solution can be also useful for the optimal deployment of public transport alternatives (such as a temporary bus line) when a disruptive event occurs on the network. By defining a set of alternative lines as an input, it is possible to find the bus routes which will provide the best network performances despite the disturbance.

By quantifying the network performance, using well-known resilience indicators, we ensure to propose the best lines combinations to be constructed in terms of efficiency and robustness. Indeed, the redundancy is characterized by the $NDC/\langle NDC \rangle$ and the efficiency by the *AE*, *NCC* and the *EBC*.

By building on our previous work (Henry et al. 2020), we relaxed the strong assumption that people could change their transportation mode an unlimited number of times, by taking transport mode shift time into account for shortest path computation. This conveys additional realism and accuracy to the REINFORCE methodology. Moreover, we consider travel demand in the selected metrics (Henry et al. 2019a), which permits to assign more importance to specific transport lines or modes that serve a larger amount of trips.

Concerning future work, the metrics used in this paper could be computed dynamically to consider the evolution of traffic conditions over time (Bellocchi and Geroliminis 2016; Tsalouchidou et al. 2020). Additionally, other kinds of metrics, such as road or

train capacity, or construction costs for additional transport segments are expected to improve the definition of the edge weights and further refine our methodology.

**Abbreviations**
REINFORCE: Rapid augmEntatIoN of large-scale multi-modal transport networks FOrResilienCe Enhancement; *NDC*: Node degree centrality; *AE*: Average efficiency; *NCC*: Node closeness centrality; *EBC*: Edge betweenness centrality; *DA*: Demand-aware; PT: Public transport; PV: Private vehicle.

**Acknowledgements**
We thank Mathieu Petit and Loïc Bonnetain who helped us with data pre-processing and preliminary analyses.

**Author Contributions**
EH, AF and N-EEF contributed to the development of the REINFORCE methodology. EH, AF and N-EEF applied the methodology on the data and analyzed the results. All authors read and approved the final manuscript.

**Funding Information**
This work has been supported by the French ANR research Project PROMENADE, Grant Number ANR-18-CE22-0008.

**Availability of data and materials**
The datasets used and/or analysed during the current study are available from the corresponding author on reasonable request.

## Declarations

**Competing interests**
The authors declare that they have no competing interests.

Received: 28 February 2021 Accepted: 26 July 2021
Published online: 23 October 2021

**References**

Aleta A, Meloni S, Moreno Y (2017) A Multilayer perspective for the analysis of urban transportation systems. Sci Rep 7(1):1–9
Aliakbary S, Habibi J, Movaghar A (2018) Quantification and comparison of degree distributions in complex networks. In: 7th international symposium on telecommunications (IST), Tehran
Aljoufie M, Zuidgeest M, Brussel M, Van Maarseveen M (2011) Urban growth and transport: understanding the spatial temporal relationship. Trans Built Environ 116:1743–3509
Altshuler Y, Puzis R, Elovici Y, Bekhor S, Pentland A (2011) Augmented betweenness centrality for mobility prediction in transportation networks. Securing Transp Syst Prot Crit Infrastruct Ser
Angelo GD, Severini L, Velaj Y (2016) On the maximum betweenness improvement problem. Electron Notes Theor Comput Sci 322:153–168
Aydin NY, Heinimann HR, Duzgun HS, Wenzel F (2018) Integration of stress testing with graph theory to assess the resilience of urban road networks under seismic hazards. Nat Hazards 91:37–68
Bellocchi L, Geroliminis N (2016) Dynamical efficiency in congested road networks. In: STRC 16th Swiss transport research conference, Monte Verita
Berche B, Von Ferber C, Holovatch T, Holovatch Y (2009) Resilience of public transport networks against attacks. Eur Phys J B 71:125–137
Bergamini E, Meyerhenke H, Crescenzi P (2018) Improving the betweenness centrality of a node by adding links. J Exp Algorithmics 23:1–32
Bíl M, Vodák R, Kubeček J, Bílová M, Sedoník J (2015) Evaluating road network damage caused by natural disasters in the Czech Republic between 1997 and 2010. Transp Res Part A Policy Pract 80:90–103
Braess D, Nagurney A, Wakolbinger T (2005) On a paradox of traffic planning. Transp Sci 39(4):446–450
Ceder A, Wilson NHM (1986) Bus network design. Transp Res Part B 20B(4):331–344
Chan R, Asce SM, Schofer JL, Asce M (2015) Measuring transportation system resilience: response of rail transit to weather disruptions. Nat Hazards Re 17:05015004
Crescenzi P, Severini L, Velaj Y (2016) Greedily improving our own closeness centrality in a network. ACM Trans Knowl Discov Data 11(1):1–32
Crucitti P, Latora V, Porta S (2006) Centrality measures in spatial networks of urban streets. Phys Rev E 73:036125
Costa LDF, Rodrigues F, Travieso G, Villas Boas PR (2007) Characterization of complex networks: a survey of measurements. Adv Phys 56(1):167–242
Dijkstra EW (1971) A short introduction to the art of programing
Dolinayova A, Zitricky V, Cerna L (2020) Decision-making process in the case of insufficient rail capacity. Sustainability (Switzerland) 12(12):6
Duan Y, Lu F (2014) Robustness of city road networks at different granularities. Stat Mech Appl Phys A 411:21–34
Eusgeld I, Kröger W, Sansavini G, Schläpfer M, Zio E (2009) The role of network theory and object-oriented modeling within a framework for the vulnerability analysis of critical infrastructures. Reliab Eng Syst Saf 94(5):954–963

Frank A, Jordán T (2015) Graph connectivity augmentation. Technical report
Freeman LC (1979) Centrality in social networks conceptual clarification. Soc Netw 2:119–141
Freiria S, Ribeiro B, Tavares AO (2015) Understanding road network dynamics: link-based topological patterns. J Transp Geogr 46(55–66):6
Gao J, Barabási A (2016) Universal resilience patterns in complex networks. Nature 530:307–312
Gauthier P, Furno A, El Faouzi N-E (2018) Road network resilience: how to identify critical linkssubject to day-to-day disruptions? Transp Res Record 2672(1):54–65
Haimes YY (2009) On the definition of resilience in systems. Risk Anal 29(4):498–501
Hassan SM, Moghaddam M, Bhouri N, Scemama G (2019) Assessment of system resilience: robustness. Reliab Redundancy Public Transp Oper
Henry E, Bonnetain L, Furno A, El Faouzi N-E, Zimeo E (2019a) Spatio-temporal correlations of betweenness centrality and traffic metrics. In: 6th international conference on models and technologies for intelligent transportation systems, Cracow University of Technology, Kraków, Poland
Henry E, Furno A, El Faouzi N-E (2019b) A graph-based approach with simulated traffic dynamics for the analysis of transportation resilience in smart cities. In: Transport research board 98th annual meeting, Washington DC
Henry E, Petit M, Furno A, Faouzi N-EE (2020) Quick sub-optimal augmentation of large scale multi-modal transport networks. In: 9th International conference on complex networks and their applications
Hitge G, Vanderschuren M (2015) Comparison of travel time between private car and public transport in Cape Town. J S Afr Inst Civ Eng 57(3):35–43
Holling CS (1973) Resilience of ecological systems. Source. Annu Rev Ecol Syst 4:1–23
International transport forum (2016) Capacity to grow: transport infrastructure needs for future trade growth. Technical report
Kazerani A, Winter S (2009) Modified betweenness centrality for predicting traffic flow. Technical report
Kivelä M, Barthelemy M, Gleeson JP, Moreno Y, Porter MA (2014) Multilayer networks
Latora V, Marchiori M (2001) Efficient behavior of small-world networks. Phys Rev 87(89):198701
Lefauconnier A (2005) Le temps de recherche d'une place de stationnement. Technical report, Ademe
Leung IXY, Chan S.-Y, Hui P, Lio' P (2011) Intra-city urban network and traffic flow analysis from GPS mobility trace
Nations U (2018) World urbanization prospects: the 2018 revision. Technical report
Porta S, Crucitti P, Latora V (2006) The network analysis of urban streets: a primal approach. Environ Plan B Plan Des 33:705–725
Puzis R, Altshuler Y, Elovici Y, Bekhor S, Shiftan Y, Pentland A (2013) Augmented betweenness centrality for environmentally aware traffic monitoring in transportation networks. J Intell Transp Syst Technol Plan Oper 17:91–105
Shalaby A, Eng P, King D (2016) Performance metrics and analysis of transit network resilience in Toronto. Transp Res Board
Tsalouchidou I, Baeza-Yates R, Bonchi F, Liao K, Sellis T (2020) Temporal betweenness centrality in dynamic graphs. Int J Data Sci Anal 9(3):257-272:4
Tu Y, Yang C, Chen X (2010) Methodology for evaluating and improving road network topology vulnerability. In: 2010 international conference on intelligent computation technology and automation. IEEE, pp 664–669
Zhang X, Miller-Hooks E, Denny K (2015) Assessing the role of network topology in transportation network resilience. J Transp Geogr 46:35–45
Zhao S, Zhao P, Cui Y (2017) A network centrality measure framework for analyzing urban traffic flow: a case study of Wuhan, China. Phys A Stat Mech Appl 478:143–157

## Publisher's Note